Theoretical Study of the Formation of Acetone in the OH-Initiated Atmospheric Oxidation of α-Pinene

L. Vereecken* and J. Peeters

Department of Chemistry, University of Leuven, Celestijnenlaan 200F, B-3001 Leuven, Belgium

Received: July 13, 2000; In Final Form: September 12, 2000

A mechanism is proposed for the formation of acetone in the OH-initiated atmospheric oxidation of α-pinene. In a first step, addition of the OH radical onto the α-pinene double bond forms a chemically activated tertiary radical P1OH†. This activated radical can then for a certain fraction break its four-membered ring, leading to a 6-hydroxymenthen-8-yl radical, which is subsequently converted to a 6-hydroxymenthen-8-oxy radical by reaction with O_2 and NO, and elimination of an NO_2 molecule. Finally, the 6-hydroxymenthen-8-oxy radical forms acetone by β C—C bond rupture. For each of these steps, competing reactions are considered, as well as the site and stereospecificity of the reaction itself. To quantify the acetone yield, quantum chemical calculations were combined with RRKM-Master Equation analyses for most of the reactions; other branching ratios were estimated from available literature data. The total yield of acetone was obtained by propagating the relevant product fractions of each step in the mechanism. We find an acetone yield of 8.5%, in good agreement with available experimental data. The uncertainty interval is estimated at 4−16%. It should be emphasized that only the nascent, chemically activated P1OH† radicals contribute to the crucial ring-breaking isomerization step.

Introduction

The global emissions of nonmethane hydrocarbons (NMHC) are dominated by biogenic compounds; for monoterpenes, a source strength exceeding 100 Tg/year is proposed.[1] These unsaturated compounds are highly reactive with ozone, OH, and nitrate radicals, with rate constants[2] for the OH reaction close to or exceeding 10^{-10} cm^3 molecule^{-1} s^{-1}, implying tropospheric lifetimes of a few hours. α-Pinene is the most widely observed monoterpene, often also with the highest emission rate. Several recent experimental studies have been performed on the OH-initiated oxidation of α-pinene,[3−6] identifying pinonaldehyde, formaldehyde, acetone, formic acid, and organic nitrates as reaction products. In these experiments, acetone yields range[3−6] from 4 to 11% in 1 atm air and at room temperature. Acetone has an atmospheric lifetime of about 15 days, sufficiently long to reach the upper troposphere and lower stratosphere, where it is believed to be a very important source of HO_x radicals.[7−9] Given the high source strength of α-pinene, its degradation could be a major source of acetone. Reaction pathways for the observed formation of acetone have been proposed;[4−5,10] however, these models all remain speculative and await experimental and theoretical affirmation.

In an attempt to elucidate the mechanism of acetone formation in the title reaction, a theoretical analysis of the OH-initiated oxidation of α-pinene was performed, combining quantum chemical methods with RRKM-Master Equation analysis to quantify the reaction kinetics of the individual steps in the mechanism. The proposed reaction scheme for acetone formation, involving four distinct consecutive reaction steps, is given in Figure 1; a detailed discussion of each step is given in the relevant section below. The first step is addition of the OH radical onto the double bond of α-pinene, forming a chemically activated tertiary adduct radical *P1OH*†, together with the isomeric secondary radical *P2OH*†; as discussed in more detail below, competition with hydrogen abstraction reactions must be taken into account, as well as the stereospecificity of the addition reactions themselves. Second, the chemically activated *P1OH*† adduct undergoes prompt isomerization reactions, in competition with collisional energy loss; depending on temperature and pressure, the strained four-membered ring will break in a (large) fraction of the activated *P1OH*† radicals, forming the more stable *6-hydroxymenthen-8-yl* radicals. In the next step, the stabilized *6-hydroxymenthenyl* radicals will rapidly react with O_2 molecules, followed by an addition of NO and elimination of NO_2, forming *6-hydroxymenthen-8-oxy* radicals. Finally, acetone can be formed from this oxy radical by β C—C bond rupture; depending on the stereochemical orientation of the OH-substituent on the six-membered ring, a 1,5-hydrogen migration can compete with the dissociation reaction.

Computational Details

To obtain accurate energetic and rovibrational data on the pertaining intermediates and transition states in the mechanism, quantum chemical geometry optimizations and frequency analyses were performed at the B3LYP-DFT/6-31G(d,p) level of theory. Vibrational wavenumbers were scaled by a factor of 0.9614, as reported by Scott and Radom[11] for the DFT/6-31G(d) level of theory. The B3LYP/6-31G(d,p) level of theory has already been validated in earlier studies on open-shell systems[12] and more specifically for β C—C bond ruptures in (hydroxy)-alkoxy radicals.[13−16] For these systems, our DFT results differed on average less than 1 kcal/mol from high-level ab initio calculations, and most often reproduced experimental barrier heights within 0.5 kcal/mol. Hence, we believe the B3LYP-DFT/6-31G(d,p) method to be in general a reliable method for the calculations presented here on a similar type reaction. Two DFT-specific problems need additional discussion. The first

* E-mail: Luc.Vereecken@chem.kuleuven.ac.be.

10.1021/jp0025173 CCC: $19.00
Published on Web 11/02/2000

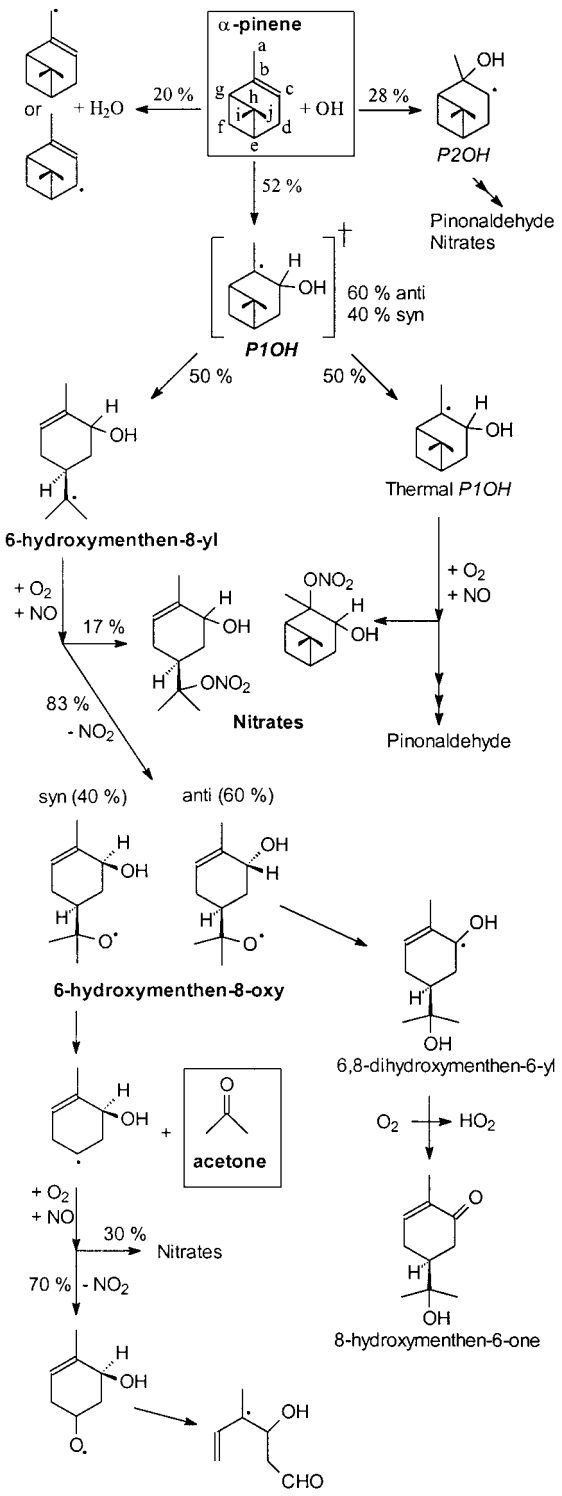

Figure 1. Reaction scheme for the formation of acetone in the OH-initiated oxidation of α-pinene.

is the reliability of the transition state energies for hydrogen shifts. DFT is reported[17−19] to underestimate these barrier heights by up to a few kilocalories per mole, though other authors[20,22] find it to give reliable results. To assess the accuracy of the B3LYP-DFT/6-31G(d,p) method, we characterized the 1-butoxy radical and its 1,5-H-shift transition state leading to 4-hydroxybutyl. The good agreement of the ZPE-corrected DFT barrier of 8.2 kcal/mol with the experimental Arrhenius activation energy[2] of 8.4 kcal/mol leads us to believe that the DFT barrier height for the analogous 1,5-H-shift in *6-hydroxymenthen-8-oxy* (see relevant section below) is also reliable. A second problem for the B3LYP-DFT/6-31G(d,p) level of theory is its inability to accurately describe very small isolated radicals, such as CH[12] and OH. The energy of the OH radical in particular is several kilocalories per mole too high, such that the exoergicity of the α-pinene + OH addition is overestimated. Due to the small basis set, the basis set superposition error (BSSE) as estimated using the Boys−Bernardi counterpoise procedure[23−24] is very large (6 kcal/mol), making the exoergicity for the α-pinene + OH addition reaction unreliable at the level of theory used. Resolving this problem requires a higher level of theory, but this is impractical at this time due to the large size of the α-pinene molecule and the need for an open-shell treatment. Unfortunately, estimating the exoergicity from analogous reactions of smaller molecules is also difficult due to the large uncertainty on the literature data. For the reaction of C_2H_4 + OH, enthalpy values reported by Atkinson et al.[25] lead to a 0 K reaction enthalpy of 28.8 kcal/mol, while the BAC-MP4 results of Melius et al.[26] yield 25.6 kcal/mol. We performed higher level ab initio calculations on the C_2H_4 + OH addition, and found (after ZPE correction) a reaction exoergicity of 25.1 kcal/mol at the B3LYP-DFT/6-311++G(2df,2pd) level of theory, 26.5 kcal/mol using G2, and 26.0 kcal/mol for G3. PMP4/6-311++G(2d,p)//MP2(full)/6-31G(d,p) and CCSD(T)/aug-cc-pVDZ//MP2(full)/6-31G(d,p) results reported by Villa et al.[27] resulted in 28.2 and 28.9 kcal/mol, respectively, prior to ZPE correction, which result in an exoergicity of 24.7 and 25.4 kcal/mol, respectively, using our B3LYP-DFT zero-point energies. All these theoretical results support the lower BAC-MP4 results of Melius et al.[26] The B3LYP-DFT results agree fairly well with the other ab initio results, so we performed additional calculations at the B3LYP-DFT/6-311++G(2df,2pd)//B3LYP-DFT/6-31G(d,p) level of theory, which is little perturbed by BSSE, describes the OH radical properly, and is still practical for somewhat larger molecules. We found 25.0 kcal/mol for the reaction enthalpy of the C_2H_4 + OH reaction, in good agreement with the other theoretical values, and 27.1 kcal/mol for the addition of OH on 2-Me-2-butene, forming 2-Me-3-hydroxy-2-butyl. This latter reaction is a good reference for the α-pinene + OH → *P1OH* addition; the higher exoergicity compared to C_2H_4 + OH is the result of the higher stability of a tertiary radical. Based on these results, we adopt a value of 27 kcal/mol for the α-pinene + OH reaction enthalpy, with an estimated error of 2 kcal/mol. The final acetone yield is only moderately sensitive to this value, changing less than 1% (absolute) per kcal/mol change in the exoergicity.

Besides addition reactions, α-pinene can also undergo hydrogen abstraction reactions. At this point, we cannot a priori calculate abstraction rates with sufficient accuracy. However, a Polanyi−Evans relation should exist between the rate of abstraction, and the abstraction reaction enthalpy, which is in turn directly related to the relevant C−H bond dissociation energy. Hence, knowledge of the C−H bond strengths can give us information as to which hydrogen is likely to be abstracted. The C−H bond dissociation energies listed in Table 1 were calculated as the difference between the parent compound, and the resulting radical after removal of a hydrogen atom, optimizing the geometry for each structure, and correcting for ZPE (see Table 2). The exact quantum chemical energy of 0.5 hartree was used for the isolated H atom; the BSSE error on the organic radical moiety is small (≤0.5 kcal/mol) and roughly the same for all compounds; it can be neglected for the present purposes. To assess the accuracy of bond dissociation energies derived in this way, the $H-CH_2CH_2CH_3$ bond strength for propane was also calculated; the resulting value of 99.6 kcal/mol (99.0 kcal/

TABLE 1: C—H Bond Dissociation Energies for a Number of Compounds and Sites, As Derived at the B3LYP-DFT/6-31G(d,p) Level of Theory

compound	radical + H	energy inc. ZPE (hartree)	C—H bond strength (kcal/mol)
propane		−119.0493955	
	1-propyl + H	−118.8907399	99.6
2-pentene		−196.4139255	
	2-penten-4-yl + H	−196.2868260	79.8
α-pinene[a]		−390.4392947	
	α-pinene-a-yl + H	−390.3076238	82.6
	α-pinene-d-yl + H	−390.3106962	80.7
	α-pinene-*g*-yl + H	−390.2764790	102.2

[a] See Figure 1 for labeling of atoms.

mol after BSSE correction) is in good agreement with the experimental value of 98 ± 1 kcal/mol.[28] Also included in Table 1 is 2-penten-4-yl as a reference compound for allyl-resonance stabilized radicals.

The Gaussian 98 progam suite[29] was used for all quantum chemical calculations. The RRKM calculations[30] and Master Equation analyses for obtaining temperature- and pressure-dependent product distributions were performed using our URESAM[31] computer program described earlier. As usual, the nascent energy distribution of the chemically activated intermediates is obtained by microreversibility considerations,[30−31] assuming Maxwell−Boltzmann energy distributions for the separated reactants. Energy specific unimolecular rate constants are calculated from our quantum chemical rovibrational data, using RRKM theory in the harmonic oscillator approximation. Collisional energy loss is incorporated using Troe's biexponential model;[32] the collision parameters needed for the *P1OH*† prompt isomerization calculations were estimated based on the experimental results[33] available for similarly sized molecules such as naphthalene and azulene at excitation levels of about 35 kcal/mol, and N_2 or O_2 as a bath gas at 300 K.

Discussion of the Reaction Mechanism

a. Initial Reaction of α-Pinene with OH Radicals. Two main channels are open to the reaction of α-pinene with OH radicals: the (barrierless) addition of the OH radical onto the double bond of α-pinene, and H-abstraction, leading to α-pinenyl + H_2O. Hydrogen abstraction has a small energy barrier, the height of which depends partly on the C—H bond strength. The rate of abstraction of alkanic hydrogens, with a bond strength of about 95−100 kcal/mol, is known to be much lower than the OH-addition rate constant on alkenes,[34−35] and therefore negligible. However, for hydrogens attached to the "a" and "d" carbons (for labeling see Figure 1), the resulting α-pinenyl radical can be stabilized by allyl resonance, reducing the C—H bond strength to about 80 kcal/mol (see Table 1) and thereby facilitating the H-abstraction. Unfortunately, no experimental data are available on the rate constants for H-abstraction from α-pinene, nor for allyl-resonance-enhanced H-abstraction in general. For α-terpinenes and α-phellandrene,[36] where the unpaired electron after H-abstraction can be delocalized over two conjugated double bonds ("super-allyl" resonance), the total H-abstraction fraction was measured to be as high as 30%, yielding an H-abstraction rate constant of 1×10^{-10} cm^3 molecule^{-1} s^{-1}.[36] The C—H bond strength for these cases is of the order of 70 kcal/mol.[37] For α-pinene, we crudely estimate that the H-abstraction rate coefficient is an order of magnitude lower. Given the total rate coefficient for the α-pinene + OH reaction, 5.4×10^{-11} cm^3 molecule^{-1} s^{-1},[2] this yields roughly a 20% hydrogen abstraction fraction, but admittedly with a large possible error of at least 10% absolute; direct experimental measurements of the H-abstraction fraction for α-pinene are in order, but difficult to carry out. Since the acetone formation mechanism put forward and theoretically quantified in the present study proceeds through OH-addition—which is thought to be the major primary route—the large uncertainty on the total contribution of the H-abstraction rate constant should affect the predicted acetone yield only moderately.

It has been suggested[5] that the hydrogen attached to the "g"-carbon in α-pinene (for labeling see Figure 1) can also be easily

TABLE 2: ZPE-Corrected Relative Energies for the Intermediates and Transition States Discussed in the Text, As Obtained at the B3LYP-DFT/6-31G(d,p) Level of Theory

structure[a]	energy (hartree)	ZPE (hartree)	relative energy (kcal/mol)
α-pinene + OH	−466.4023181	0.244597	29.6[b]
syn-*P1OH*	−466.4546731	0.250166	0.1
anti-*P1OH*	−466.4549228	0.250251	0.0
syn-*P2OH*	−466.4542971	0.249862	0.2
anti-*P2OH*	−466.4529961	0.249956	1.0
anti-*P1OH*	−466.4546731	0.250166	0.0
anti-*6-hydroxymenthen-8-yl*	−466.4717509	0.248643	−11.6
anti-*Rad3*	−466.4696089	0.250320	−9.3
anti-*Rad4*	−466.4616231	0.245999	−6.9
anti-*Rad5*	−466.4453460	0.248036	4.6
anti-*Rad6*	−466.4620580	0.248902	−5.4
anti-*Rad7*	−466.4598730	0.247950	−4.6
anti-*Rad8*	−466.4735597	0.250381	−11.7
anti-*Rad9*	−466.4606101	0.246647	−5.9
anti-*Rad10*	−466.4574541	0.247366	−3.4
anti-*Rad11*	−466.4642207	0.248820	−6.8
anti-*TS1*	−466.4331090	0.248008	12.2
anti-*TS2*	−466.4263477	0.245416	14.9
anti-*TS3*	−466.4338724	0.248261	11.9
anti-*TS4*	−466.4095538	0.247782	26.9
anti-*TS5*	−466.4090074	0.245189	25.7
anti-*TS6*	−466.4394926	0.248350	8.4
anti-*TS7*	−466.4247611	0.247620	17.2
anti-*TS8*	−466.4239123	0.245503	16.5
anti-*TS9*	−466.4290167	0.247853	14.7
anti-*TS10*	−466.4142785	0.247427	23.7
anti-*TS11*	−466.4155247	0.245023	21.5
anti-*TS12*	−466.4449254	0.248360	5.0
syn-*P1OH*	−466.4549228	0.250251	0.0
syn-*6-hydroxymenthen-8-yl*	−466.4720823	0.249016	−11.5
syn-*Rad3*	−466.4698618	0.250246	−9.4
syn-*Rad4*	−466.4627245	0.245877	−7.5
syn-*Rad6*	−466.4633076	0.248921	−6.1
syn-*Rad7*	−466.4598915	0.247753	−4.6
syn-*Rad8*	−466.4728823	0.250633	−11.0
syn-*Rad10*	−466.4579632	0.247413	−3.6
syn-*Rad11*	−466.4626688	0.248875	−5.7
syn-*TS1*	−466.4345787	0.248290	11.6
syn-*TS2*	−466.4278390	0.245842	14.3
syn-*TS3*	−466.4349374	0.248368	11.4
syn-*TS4*	−466.4115901	0.247869	25.8
syn-*TS5*	−466.4127126	0.245676	23.7
syn-*TS6*	−466.4395670	0.248442	8.5
syn-*TS7*	−466.4250599	0.247763	17.2
syn-*TS8*	−466.4238993	0.245434	16.6
syn-*TS9*	−466.4275048	0.247907	15.8
syn-*TS10*	−466.4143759	0.245159	22.4
syn-*TS11*	−466.4130567	0.247373	24.5
syn-*TS12*	−466.4434893	0.248219	6.0
anti-*6-hydroxymenthen-8-oxy*	−541.6780204	0.253964	0.0
1,5-H shift TS	−541.6707730	0.250899	2.7
acetone elimination TS	−541.6639806	0.251693	7.4

[a] See Figure 2 for the compounds corresponding to each name (the geometry optimalization for syn-*Rad5* and syn-*Rad9* did not converge in time for this publication). [b] Becomes 23.5 kcal/mol after BSSE correction. A value of 27 kcal/mol is used for the kinetic calculations (see text).

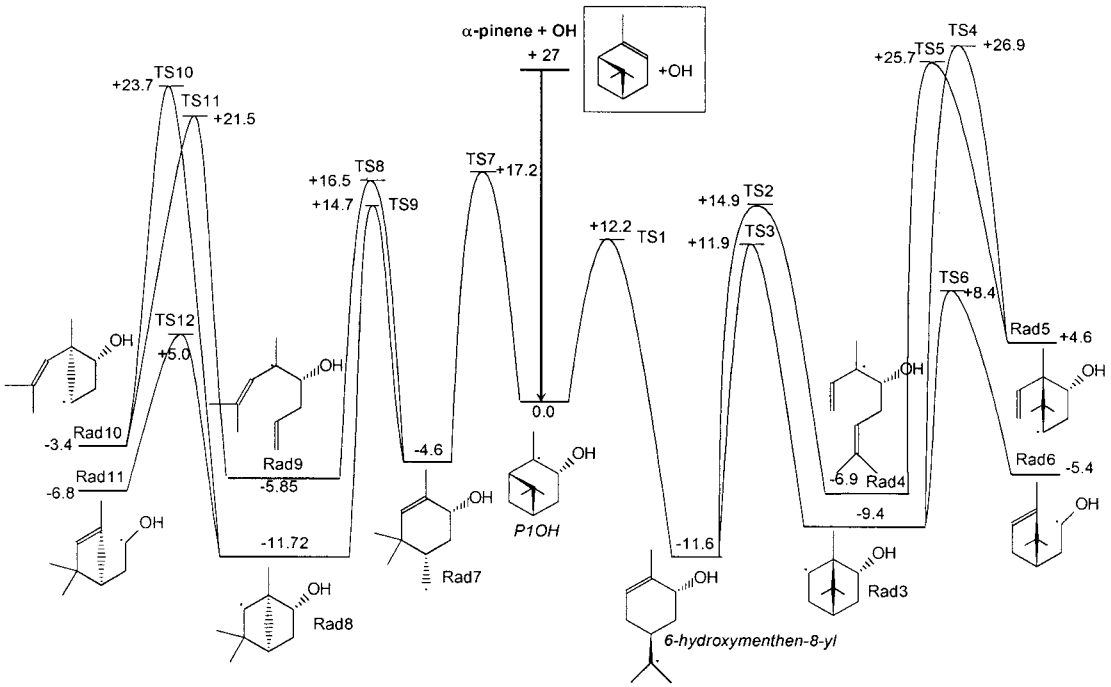

Figure 2. B3LYP-DFT/6-31G(d,p) potential energy surface for the isomerization of *P1OH*, formed in the reaction of α-pinene + OH. Energies are expressed in kcal/mol and corrected for ZPE energy. The given PES is for anti-addition on the double bond; the energies for syn-addition differ by about 1 kcal/mol (see Table 2). For structures with internal rotations, only one (local) minimum was optimized; lower-lying conformers might exist which are usually within 2−3 kcal/mol of each other.

abstracted, assuming an allyl-resonance stabilization, and this pathway was invoked to explain the observed acetone formation.[5] However, our quantum chemical calculations (see Table 1) show that this allyl resonance does not occur at all; the strained ring structure prohibits sp2 hybridization for the "g" carbon, such that the radical orbital cannot assume the required spatial attitude with respect to the double bond. Therefore, the unpaired electron remains localized on the "g" carbon, thereby somewhat increasing the four-membered ring strain, and the C−H bond strength of 102 kcal/mol is therefore even larger than a normal alkane C−H bond. This indicates that abstraction of this hydrogen will not be an important reaction channel.

Addition of OH onto the α-pinene double bond, occurring for ∼80%, leads to *P1OH*, a tertiary radical, or *P2OH*, a secondary radical, depending on the addition site (see Figure 1). According to a site-specific structure−activity relationship for alkene + OH reactions,[38−39] the branching ratio *P1OH*/*P2OH* for tertiary/secondary addition sites is expected to be 55/30. The predictions of this SAR—which should be applicable to this case also—agree within 5−10% (absolute) of the product distributions measured directly for a number of alkenes.[39] Besides the site-specificity, there is also the stereospecificity of syn- or anti-addition of the OH on the ring, with the syn-position defined as the side with the $-C(CH_3)_2-$ bridge. The stereochemistry will become important later, so this aspect must be taken into account. Addition in syn-position is likely to be somewhat sterically hindered relative to the anti-side due to the presence of the methyl substituents on the bridge. Unfortunately, no data on the ratio of syn/anti are available, so we estimate the syn/anti ratio for *P1OH* at 40/60, with an estimated absolute error of 10%. The fate of the *P2OH* adduct is not discussed further here since it does not offer any easily accessible acetone formation routes; it will mainly form pinonaldehyde and nitrates through the usual reactions.

b. Reactions of Chemically Activated *P1OH*†. Figure 2 shows the B3LYP-DFT/6-31G(d,p) potential energy surface for unimolecular isomerization reactions starting from *P1OH*†. The most important isomerization reaction for *P1OH* in the context of this article is the breaking of the four-membered ring, leading to *6-hydroxymenthen-8-yl*, with a calculated barrier height of 12.2 kcal/mol. This low barrier height is due to the strain in the four-membered ring of about 27 kcal/mol,[40] and the formation of a double bond in 6-*hydroxymenthen-8-yl*. To assess the accuracy of our theoretical barrier height, it can be compared to the barrier height of the analogous ring breaking in cyclobutylmethyl radicals, which has been listed[41] for use as a calibrated radical clock reaction: $k(T) = 4 \times 10^{12} \exp(-12.2 \text{ kcal mol}^{-1}/RT)$, and $k(298 \text{ K}) = 5 \times 10^3 \text{ s}^{-1}$.

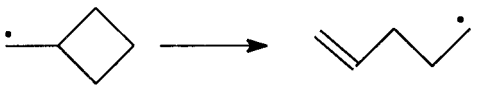

An Arrhenius expression was derived for the *P1OH* → 6-*hydroxymenthen-8-yl* ring breaking, based on rate constants as obtained by Transition State Theory calculations using our quantum chemical rovibrational data: $k_{open}(T) = 1.9 \times 10^{13} \exp(-12.8 \text{ kcal mol}^{-1}/RT)$. The Arrhenius activation energy, $E_a = 12.8$ kcal/mol, is in good agreement with that for the reference cyclobutylmethyl radical ring opening, 12.2 kcal/mol. We therefore estimate an uncertainty of about 0.5 kcal/mol on the barrier height of the TS for ring breaking. The four-membered ring in *P1OH* can also be broken on the opposite side, yielding *Rad7*. This reaction is energetically more difficult, due to the tertiary radical being converted to a primary radical, and is therefore only a very minor channel. As discussed further below, the remaining isomerization channels are of negligible importance in the context of the acetone formation in atmospheric conditions (1 atm), and will not be discussed in more detail.

From the Arrhenius expression given above we derive the thermal rate coefficient of isomerization of *P1OH* to *6-hydroxymenthen-8-yl* at 300 K: $k_{open}(300 \text{ K}) = 8 \times 10^3 \text{ s}^{-1}$, very close to the experimental value for cyclobutylmethyl given above. The reaction of *P1OH* + O_2, with an estimated pseudo-first-

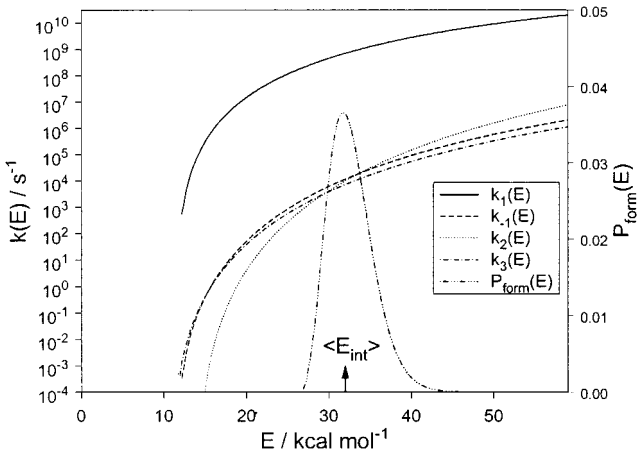

Figure 3. $<E_{int}>$ indicates the average nascent internal energy of the *P1OH*† radicals; it is obtained from the depicted normalized *P1OH*† nascent energy distribution $P_{form}(E)$ (expressed as fractions per energy bin of size 0.24 kcal/mol). $k_1(E)$ represent the energy-specific unimolecular rate constants for the *P1OH* → *6-hydroxymenthen-8-yl* isomerization reaction. k_{-1}, k_2, and k_3 are the energy-specific rate constants for isomerization of *6-hydroxymenthen-8-yl* through *TS1*, *TS2*, and *TS3*, respectively (see Figure 2). All energies are relative to the ground-state energy of *P1OH*.

order rate coefficient in 1 atm air of $k_{P1OH+O2} = 5 \times 10^7$ s^{-1},[25] would easily outrun the thermal isomerization, making isomerization a nonissue. However, the exothermic OH addition reaction leads to the formation of chemically activated *P1OH*† adducts; their high initial internal energy content of 32 kcal/mol, comprising 27 kcal/mol exoergicity plus 5 kcal/mol on average of thermal energy inherited from the reactants, allows them to quickly undergo isomerization reactions which under thermal conditions would be too slow. As these "prompt", chemically activated isomerization reactions must compete with collisional energy loss, the product distribution for the α-pinene + OH reaction depends strongly on pressure. At very high pressures, the rate of stabilization outruns the isomerization, and only thermal *P1OH* radicals will be formed which will subsequently react with O_2. In contrast, at low pressures, collisional energy loss will be slow and a high number of different compounds can be formed. This effect has been observed by Vinckier et al.[10] for pressures of a few Torr, using He as a bath gas: in these reaction conditions a bewildering array of products was observed, most of which disappeared[42] on increasing the pressure to 50 Torr.

For normal atmospheric boundary layer conditions, 1 atm of air and 298 K, we find a falloff behavior in which only the first isomerization reaction has a significant chance of occurring before collisional energy loss. To quantify the amount of prompt isomerization we performed RRKM-Master Equation analyses on this system, using the DFT rovibrational data and ZPE-corrected energies. Collision parameters used for *P1OH* and isomers were $\sigma_{A-A} = 8.0$ Å, $\epsilon/k = 600$ K, and $<-\Delta E_{tot}> = 100-125$ cm^{-1}. This results in a theoretical product distribution of 50% formation of 6-*hydroxymenthen-8-yl*, and 50% thermalized *P1OH*, with negligible fractions (<1%) of other compounds. The differences between the quantum chemical characteristics for the syn- and anti-isomers is sufficiently small to treat both stereoisomers as being identical. The energy-specific rate constants $k_1(E)$ for the *P1OH* → 6-*hydroxymenthen-8-yl* isomerization reactions are given in Figure 3, as well as the nascent energy distribution of *P1OH*†. The steady-state population at 1 atm is shifted downward compared to the nascent distribution due to collisional energy loss, such that the population-averaged prompt isomerization rate constant at 1 atm becomes 2×10^8 s^{-1}. Also depicted in Figure 3 are the energy-specific rate constants $k(E)$ for the 6-*hydroxymenthen-8-yl* isomerizations; at 1 atm these prompt isomerization reactions, with population-averaged rate constants $< 3 \times 10^3$ s^{-1}, are not competitive with collisional energy loss. The obtained product distribution is mainly sensitive to the uncertainty of the barrier height of ring breaking (±7% absolute for the uncertainty of ±0.5 kcal/mol), the exoergicity of the addition reaction (±10% absolute for the ±2 kcal/mol uncertainty), and the transferred energy $<\Delta E_{tot}>$ per collision with the bath gas (5% change absolute over the 100−125 cm^{-1} range), leading to an aggregate uncertainty of 50 ± 15% on the obtained product distribution. The fate of the thermalized *P1OH* radicals will not be discussed further here; similar to *P2OH*, they are expected to lead mainly to nitrates and pinonaldehyde. As already mentioned, the yield of 6-*hydroxymenthen-8-yl* should increase at lower pressures, due to a lower stabilization rate and hence more available time for prompt isomerization. At 2 Torr, Vinckier et al.[43] measured an acetone yield of 18%, substantially larger than the yields found at 1 atm, consistent with our proposed acetone formation route proceeding through the prompt isomerization of *P1OH*† to 6-*hydroxymenthen-8-yl* in competition with collisional stabilization.

c. Reactions of *6-Hydroxymenthen-8-yl*. The 6-*hydroxymenthen-8-yl* radical will react very rapidly with O_2, forming the corresponding *6-hydroxymenthenyl-8-peroxy* radical. In atmospheric conditions with NO present, this peroxy radical will quickly react to a 6-*hydroxymenthenyl-8-peroxynitrite*, which for a minor fraction will isomerize to form nitrates. No data are available on this fraction of nitrate formation for this compound, but it can be estimated from the structure−activity relation given by Atkinson:[2] for a tertiary C_{10}-peroxynitrite, 17% of nitrate formation is expected. The major part of the peroxynitrite molecules will dissociate to 6-*hydroxymenthen-8-oxy* radicals + NO_2.

d. Reactions of the *6-Hydroxymenthen-8-oxy* Radical. Two important unimolecular reaction channels are accessible to the 6-*hydroxymenthen-8-oxy* radicals formed in the earlier reaction steps. The first is β C−C bond cleavage, leading to acetone. The barrier height for this dissociation reaction was calculated at 7.4 kcal/mol; Transition State Theory calculations using the B3LYP/6-31G(d,p) rovibrational data for this process yield a thermal rate constant of $k_{acetone}(300\ K) = 2.4 \times 10^7$ s^{-1}; this level of theory has been used earlier to calculate rates of alkoxy radical decomposition,[13−15] yielding results in very good agreement with available experimental data. The second unimolecular reaction applies only to the 60% *6-hydroxymenthen-8-oxy* radicals with the OH in anti-position: for this stereochemistry, the possibility of a 1,5 H-shift exists, forming *6,8-dihydroxymenthen-6-yl*. This hydrogen shift has only a low barrier: due to the flexibility of the six-membered ring and the free internal rotation of the $-C(CH_3)_2O$ substituent, virtually no strain is needed to position the oxy-group close to the migrating hydrogen, and the exoergicity is very large (estimated at ≈20−25 kcal/mol) owing to the presence of the α-hydroxy functionality in the primary reactant radical and the allyl resonance of the tertiary product radical. All other hydrogen shift reactions conceivable in both the syn- and anti-isomer will have much higher energy barriers, due to the less stable reaction products and the geometrically strained transition states. The B3LYP-DFT barrier height for the 1,5 H-shift is only 2.7 kcal/mol, resulting in a TST rate constant for the thermal H-shift in *anti-6-hydroxymenthen-8-oxy* of $k_{shift}(300\ K) = 1.2 \times 10^{10}$ s^{-1}. For the anti-isomer, therefore, hydrogen shift will always outrun

the formation of acetone. The barrier height for the 1,5 H-shift is not a sensitive parameter here; even if it were severely underestimated by over 2 kcal/mol, isomerization would still be much faster than dissociation: assuming un upper limit for the H-shift barrier height of 5 kcal/mol, we find a lower-limit TST rate constant for the thermal H-shift in *anti-6-hydroxymenthen-8-oxy* of $k_{shift}(300\ K) \geq 2.5 \times 10^8\ s^{-1}$, still over an order of magnitude faster than the dissociation reaction. Due to the high reaction exoergicity, the reverse isomerization of *6,8-dihydroxymenthen-6-yl* to *6-hydroxymenthen-8-oxy* is unimportant. Bimolecular reactions of the 6-*hydroxymenthen-8-oxy* radical are not competitive with the unimolecular processes: reaction with O_2 -usually a major sink for alkoxy radicals- is negligible here due to the lack of an α-hydrogen next to the oxy substituent, and other bimolecular reactions are too slow to compete with the unimolecular reactions. On the basis of these considerations we conclude that the *syn-6-hydroxymenthen-8-oxy* isomer will dissociate all of the time to form acetone, whereas the anti-isomer will form almost exclusively the 6,8-*dihydroxymenthen-6-yl* radical.

e. Further Reactions. After acetone loss from the *syn-6-hydroxymenthen-8-oxy* radical, a substituted cyclohexenyl radical remains, which will react rapidly with O_2 and NO. The resulting cyclohexenylperoxynitrite will either isomerize to an organic nitrate, or will lose an NO_2 molecule, forming a cyclohexenoxy radical. For a secondary C_{10}-peroxynitrite, the structure−activity relationship proposed by Atkinson[2] predicts a 60% dissociation fraction, leaving 40% of organic nitrates. Breaking of the six-membered ring in the oxy radical is predicted to be a facile process, due to the allyl-resonance stabilization of the products.

The *6,8-dihydroxymenthen-6-yl* radicals, formed after an H-shift in *anti-6-hydroxymenthen-8-oxy*, will most likely react with O_2, leading to *8-hydroxymenthen-6-one* + HO_2. It is interesting to note at this point that this hydroxycarbonyl compound has the same molecular weight as pinonaldehyde. Assuming 6,8-*dihydroxymenthen-6-yl* always reacts with O_2, we obtain an estimated yield of 10% for 8-*hydroxymenthen-6-one*, which could interfere in determinations of pinonaldehyde yields.

Conclusions

The total yield of acetone in the OH-initiated tropospheric oxidation of α-pinene can be obtained by propagating the probabilities for each of the reactions steps discussed above, resulting in 8.5% of acetone, in very good agreement with the experimental data. Propagating the upper and lower limits of the yields at each reaction step leads to a 4−16% interval. The mechanism proposed in this article as given in Figure 1, is supported by high-level quantum chemical data, RRKM-based Master Equation analyses, Transition State Theory calculations, and available literature data. The most important new elements are the prompt isomerization of the initial $P1OH^{\dagger}$ adduct, and the explicit consideration of the stereospecificity for the OH-addition. The mechanism is consistent with the experimentally observed primary acetone formation from α-pinene, both at 1 atm and lower pressures.

Supporting Information Available: Cartesian coordinates, rotational constants, and vibrational wavenumbers of the minima and transition states relevant to the acetone formation from α-pinene. This material is available free of charge via the Internet at http://pubs.acs.org.

Note Added in Proof. Vinckier et al. (unpublished results) recently detected and identified 8-hydroxymenthen-6-one as a product in the OH-initiated α-pinene oxidation at low pressures, using the 2,4-DNPH derivatization method for ketones and aldehydes, followed by HPLC-MS analysis.

Acknowledgment. Financial support of the Fonds voor Wetenschappelijk Onderzoek, Flanders, and of the Bijzonder Onderzoeksfonds, Flanders, is gratefully acknowledged.

References and Notes

(1) Guenther, A.; Hewitt, C. N.; Erickson, D.; Fall, R.; Geron, C.; Graedel, T.; Harley, P.; Klinger, L.; Lergau, M.; McKay, W. A.; Pierce, T.; Scholes, B.; Steinbrecher, R.; Tallamraju, R.; Taylor, J.; Zimmerman, P. *J. Geophys. Res.* **1995**, *100*, 8873.

(2) Atkinson, R. *J. Phys. Chem. Ref. Data* **1997**, *26*, 215.

(3) Orlando, J. J.; Nozière, B.; Tyndall, G. S.; Orzechowska, G. E.; Paulson, S. E.; Rudich, Y. *J. Geophys. Res*. Submitted for publication.

(4) Nozière, B.; Barnes, I.; Becker, K.-H. *J. Geophys. Res.* **1999**, *104*, 23645.

(5) Aschmann, S. M.; Reissell, A.; Atkinson, R.; Arey, J. *J. Geophys. Res.* **1998**, *103*, 553.

(6) Fantechi, G. Ph.D. Thesis, KULeuven, 1999.

(7) Singh, H. B.; O'Hara, D.; Herlth, D.; Sachse, W.; Blake, D. R.; Bradshaw, J. D.; Kanakidou, M.; Crutzen P. J. *J. Geophys. Res*. **1994**, *99*, 1805.

(8) Singh, H. B.; Kanakidou, M.; Crutzen, P. J.; Jacob, D. J. *Nature* **1995**, *378*, 50.

(9) McKeen, S. A.; Gierczak, T.; Burkholder, J. B.; Wennberg, P. O.; Hanisco, T. F.; Keim, E. R.; Gao, R. S.; Liu, S. C.; Ravishankara, A. R.; Fahey, D. W. *Geophys. Res. Lett*. **1997**, *24*, 3177.

(10) Vinckier, C.; Compernolle, F.; Saleh, A. M. *Bull. Soc. Chim. Belg*. **1997**, *106*, 501.

(11) Scott, A. P.; Radom, L. *J. Phys. Chem*. **1996**, *100*, 16502.

(12) Vereecken, L.; Pierloot, K.; Peeters, J. *J. Chem. Phys*. **1998**, *108*, 1068.

(13) Orlando, J. J.; Tyndall, G. S.; Bilde, M.; Ferronato, C.; Wallington, T. J.; Vereecken, L.; Peeters, J. *J. Phys. Chem. A* **1998**, *102*, 8116.

(14) Vereecken, L.; Peeters, J. *J. Phys. Chem. A* **1999**, *103*, 1768.

(15) Vereecken, L.; Peeters, J.; Orlando, J. J.; Tyndall, G. S.; Ferronato, C. *J. Phys. Chem. A* **1999**, *103*, 4693.

(16) Orlando, J. J.; Tyndall, G. S.; Vereecken, L.; Peeters, J. *J. Phys. Chem. A*, submitted for publication.

(17) Johnson, B. G.; Gonzales, C. A.; Gill, P. M. W.; Pople, J. A. *Chem. Phys. Lett*. **1994**, *221*, 100.

(18) Durant, J. L. *Chem. Phys. Lett.* **1996**, *256*, 595.

(19) Nguyen, M. T.; Creve, S.; Vanquickenborne, L. G. *J. Chem. Phys*. **1996**, *105*, 1922.

(20) Skokov, S.; Wheeler, R. A. *Chem. Phys. Lett*. **1997**, *271*, 251.

(21) Basch, H.; Hoz, S. *J. Phys. Chem. A* **1997**, *101*, 4416.

(22) Susnow, R. G.; Dean, G. M.; Green, W. H., Jr. *Chem. Phys. Lett*. **1999**, *312*, 262.

(23) Boys, S. F.; Bernardi, F. *Mol. Phys*. **1970**, *19*, 553.

(24) Van Duijneveldt, F. B.; Van Duijneveldt-van de Rijdt, C. M.; Van Lenthe, J. H. *Chem. Rev.* **1994**, *94*, 1873.

(25) Atkinson, R.; Baulch, D. L.; Cox, R. A.; Hampson, R. F., Jr.; Kerr, J. A.; Rossi, M. J.; Troe, J. *J. Phys. Chem. Ref. Data* **1997**, *26*, 521.

(26) Melius, C. F. *BAC-MP4 Heats of Formation and Free Energies*; Sandia National Laboratories: Livermore, CA, 1996.

(27) Villà, J.; González-Lafont, A.; Lluch, J. M.; Corchado, J. C.; Espinosa-García, J. *J. Chem. Phys*. **1997**, *107*, 7266.

(28) *CRC Handbook of Chemistry and Physics*; Weast, R. C., Astle, M. J., Eds.; CRC Press Inc.: Boca Raton,FL,

(29) Frisch, M. J.; Trucks, G. W.; Schlegel, H. B.; Scuseria, G. E.; Robb, M. A.; Cheeseman, J. R.; Zakrzewski, V. G.; Montgomery, J. A., Jr.; Stratmann, R. E.; Burant, J. C.; Dapprich, S., Millam, J. M.; Daniels, A. D.; Kudin, K. N.; Strain, M. C.; Farkas, O.; Tomasi, J.; Barone, V.; Cossi, M.; Cammi, R.; Mennucci, B.; Pomelli, C.; Adamo, C.; Clifford, S.; Ochterski, J.; Petersson, G. A.; Ayala, P. Y.; Cui, Q.; Morokuma, K.; Malick, D. K.; Rabuck, A. D.; Raghavachari, K.; Foresman, J. B.; Cioslowski, J.; Ortiz, J. V.; Stefanov, B. B.; Liu, G.; Liashenko, A.; Piskorz, P.; Komaromi, I.; Gomperts, R.; Martin, R. L.; Fox, D. J.; Keith, T.; Al-Laham, M. A.; Peng, C. Y.; Nanayakkara, A.; Gonzalez, C.; Challacombe, M.; Gill, P. M. W.; Johnson, B.; Chen, W.; Wong, M. W.; Andres, J. L.; Gonzalez, C.; Head-Gordon, M.; Replogle, E. S.; Pople, J. A. *Gaussian 98, Revision A*.5; Gaussian, Inc., Pittsburgh, PA, 1998.

(30) Forst, W. *Theory of Unimolecular Reactions*; Academic Press: New York, 1973.

(31) Vereecken, L.; Huyberechts, G.; Peeters, J. *J. Chem. Phys*. **1997**, *106*, 6564.

(32) Troe, J. *J. Chem. Phys*. **1977**, *66*, 4745.

(33) Oref, I.; Tardy, D. C. *Chem. Rev.* **1990**, *90*, 1407.

(34) Atkinson, R. *Chem. Rev.* **1985**, *85*, 69.

(35) Atkinson, R. *J. Phys. Chem. Ref. Data, Monograph 2* **1994**, 1−216.

(36) Peeters, J.; Vandenberk, S.; Piessens, E.; Pultau, V. *Chemosphere* **1999**, *38*, 1189.

(37) Vereecken, L.; Peeters, J. *Chem. Phys. Lett.*, submitted, 2000.

(38) Peeters, J.; Boullart, W.; Van Hoeymissen, J. *Proceedings of EUROTRAC Symposium '94*; Borell, P. M., et al., Eds.; SPB Academic Publishing: The Hague, 1994; pp 110−114.

(39) Peeters, J.; Boullart, W.; Pultau, V.; Vandenberk S. *Proceedings of EUROTRAC Symposium '96*; Borell, P. M., et al., Eds.; Computational Mechanics Publications: Southampton, 1996; pp 471−475.

(40) Pedley, J. B. *Thermochemical Data and Structures of Organic Compounds*; Thermodynamics Research Center Data Series: Texas, 1994.

(41) Newcomb, M. *Tetrahedron* **1993**, *49*, 1151.

(42) Van den Bergh, V.; Vanhees, R.; De Boer, R.; Compernolle, F.; Vinckier, C. *J. Cromatogr. A*, accepted for publication.

(43) Vinckier, C.; Compernolle, F.; Saleh, A. M.; Van Hoof, N.; Van Hees, I. *Fresenius Environ. Bull.* **1998**, *7*, 361.